Geochemical Journal, Vol. 50, pp. 357 to 362, 2016 doi:10.2343/geochemj.2.0420

NOTE

Carbonate preservation during the 'mystery interval' in the northern Indian Ocean

SUSHANT S. NAIK* and P. DIVAKAR NAIDU

CSIR-National Institute of Oceanography, Dona-Paula, Goa 403004, India

(*Received November 17, 2015; Accepted March 12, 2016*)

To understand carbonate dissolution and/or preservation on the sea floor since the Last Glacial Maximum (LGM), we measured shell weights of planktonic foraminifera *Globigerinoides ruber* from four sediment cores retrieved from different water depths (~800 to 3300 m) across the northern Indian Ocean. *G. ruber* shell weight pattern shows an overall decrease starting from the LGM, with a spike, also termed as the 'mystery interval', during the early deglaciation (~17.5 to 14.5 ka). This shell weight maximum is a feature noted across the world oceans and considered to signify carbonate preservation, although it is missing from many sediment cores from the eastern equatorial Pacific, tropical Atlantic and subtropical Indian Ocean. The carbonate preservation spike during deglaciation in the northern Indian Ocean documented in this study suggests increased deep-water carbonate ion concentrations during the early deglaciation which in turn favored preservation. This study sheds new light on the preservation of carbonate and associated deep water circulation during deglaciation in the northern Indian Ocean.

Keywords: mystery interval, deglaciation, shell weights, northern Indian Ocean, ventilation

INTRODUCTION

We know from ice-core records that atmospheric CO_2 showed a cyclicity of ~100 kyr, with eight known cycles where the CO_2 varied within a range of 180 to 280 ppmv (Luthi *et al.*, 2008). The increase of atmospheric CO_2 from the Last Glacial Maximum (LGM) to the Holocene accelerated during deglaciation (Marcott *et al.*, 2014). These glacial-interglacial atmospheric CO_2 variations are thought to be regulated by the oceans. Atmospheric CO_2 levels during glaciation were lower due to the isolation of the deep water masses from the atmosphere by increased stratification (e.g., Sigman and Boyle, 2000). The rapid rise in atmospheric CO_2 during deglaciation (~17 to 11 ka) was a result of breakdown of this stratification and increased deep-ocean ventilation releasing CO_2 that was stored in the deep ocean to the atmosphere. This is also called the ventilation hypothesis (Anderson *et al.*, 2009). Across the planet, the early deglaciation (~17.5 to 14.5 ka) saw mutually contradictory climatic response and was hence termed the 'mystery interval' (Denton *et al.*, 1999). During this interval, a temporary maximum in $CaCO_3$ preservation in deep-sea sediments was observed (Berger, 1977). However, this preservation spike is missing in several sediment cores from the world oceans (Mekik *et al.*, 2012). In order to observe whether the preservation of carbonate observed mainly in the Atlantic and Pacific was also evident in the less studied region of the northern Indian Ocean, we measured shell weights from sediment cores covering the last ~25 kyr with a special emphasis on the early deglacial period (~17.5 to 14.5 kyr).

STRATEGY

The reaction of CO_2 with seawater causes a change in its carbonate chemistry. This carbonate chemistry is of utmost importance to shell forming organisms like foraminifera that secrete a $CaCO_3$ shell. As the concentration of dissolved CO_2 in seawater increases, the pH of seawater is reduced, as is the concentration of the carbonate ions necessary for shell build up. These conditions result in a reduction in the calcification process. However, apart from this major control there are other factors that may affect shell calcification. These may include; 1) the presence of symbionts (Rink *et al.*, 1998), 2) photosynthesis, 3) the availability of light, 4) variation in genotype and 5) the presence of optimal growth conditions.

As shells sink after the death of the organism, they settle on the seafloor. Two processes cause the dissolu-

*Corresponding author (e-mail: sushant@nio.org)

Table 1. Cores used in the present study showing average shell weights during LGM (18–24 kyr), deglaciation (11–17 kyr) and Holocene (0–11 kyr). The shell weights for these time periods were averaged within respective cores.

Core	Latitude	Longitude	Chronology (number of AMS ^{14}C age-points)	Water depth (m)	Holocene shell weights (μg)	Deglacial shell weights (μg)	LGM shell weights (μg)
ODP 723	18°03′ N	57°37′ E	13 (Naidu and Niitsuma, 2004)	808	15.1	16.2	14.0
AAS 9/21	14°30′ N	72°39′ E	5 (Govil and Naidu, 2010)	1807	14.0	14.9	14.6
SK 157/20	12°09′ N	88°42′ E	5	3171	13.3	15.5	—
SK 218	14°02′ N	82°00′ E	6 (Govil and Naidu, 2011)	3307	15.9	17.6	16.7

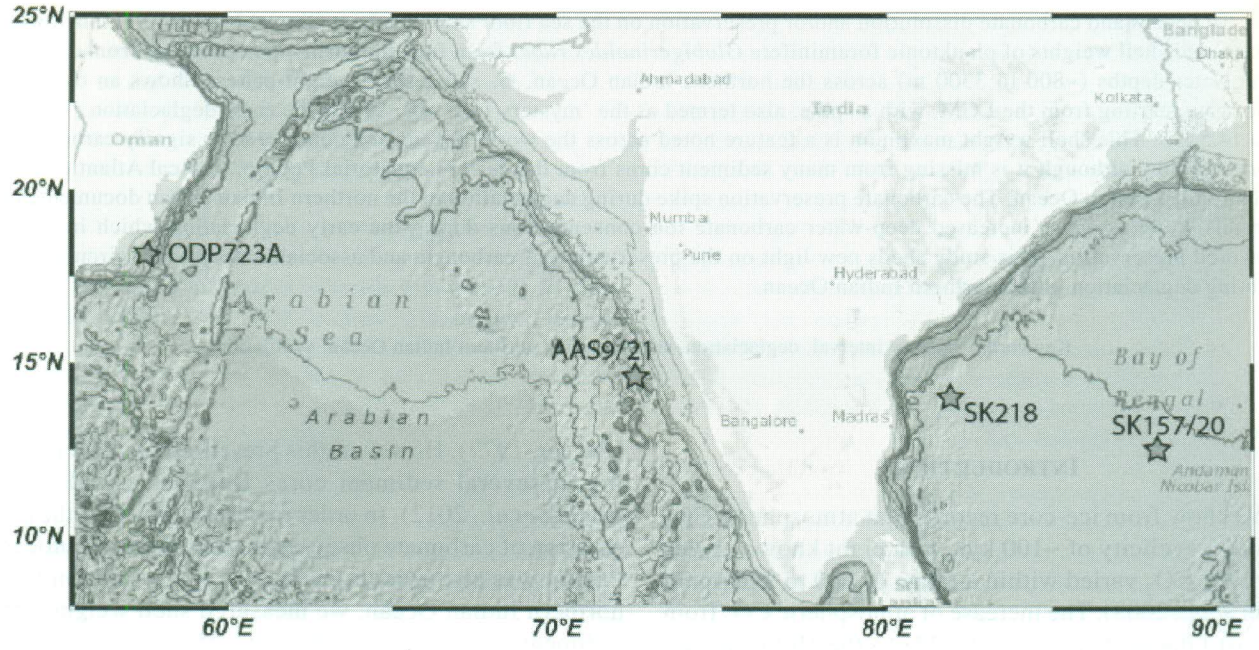

Fig. 1. Core locations in the northern Indian Ocean (map courtesy: Bathymetric Data Viewer, NOAA).

tion of calcite after it reaches the seafloor. First, the concentration of CO_3^{2-} in the seawater close to the seafloor (Berger, 1973), and second, sedimentary organic matter respiration and the resulting acidification of pore waters (Emerson and Bender, 1981; Archer and Maier-Reimer, 1994). The shell weights of foraminifera from a narrow range of shell sizes can provide a measure of the extent of dissolution (Lohmann, 1995).

Samples and Methods

The sediment cores used in this study were obtained from the northern Indian Ocean (Table 1 and Fig. 1). All the samples were oven dried at 50°C, after which a portion of each sample was weighed, disaggregated by soaking in distilled water, and then wet sieved through a >63 μm sieve. For shell weight measurements, the coarse material was further sieved in the size range of 300–355 μm. Approximately 30 *Globigerinoides ruber* (white) shells were picked from this size fraction using a Stereo-zoom binocular microscope, and subsequently weighed on a microbalance (1σ precision: ± 1 μg, $n = 10$). Shell weights for cores ODP 723A and AAS 9/21 have been published previously (Naik and Naidu, 2014).

The AMS ^{14}C dating for SK 157/20 was performed on mono-specific samples of the planktonic foraminifera *G. ruber* using the Tandem Accelerator at Leibniz Labor für Altersbestimmung und Isotopenforschung, Christian-Albrechts-Universität, Kiel, Germany and Arizona AMS Facility, USA. Radiocarbon ages were calibrated to calendar years using the calibration program (CALIB 6.0) of Stuiver and Reimer (1993). For the $\delta^{13}C$ analyses on

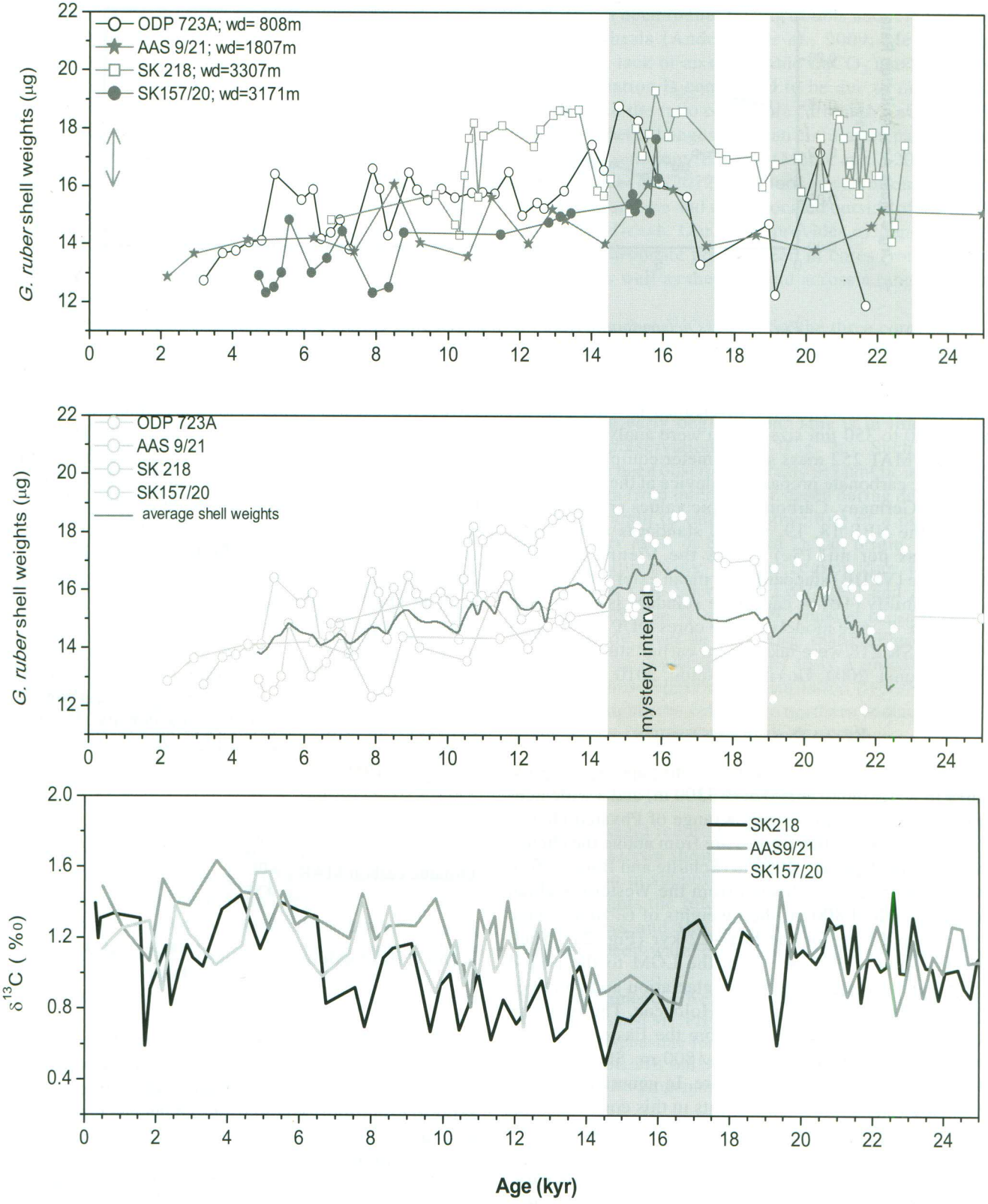

Fig. 2. a) Shell weights in general show a decreasing trend for all the four sediment cores through time, b) averaged shell weights for the four cores show a deglacial spike (averaging multiple trends using the 'origin' software) and c) $\delta^{13}C$ record for AAS 9/21 and SK 218 show lower values during deglaciation.

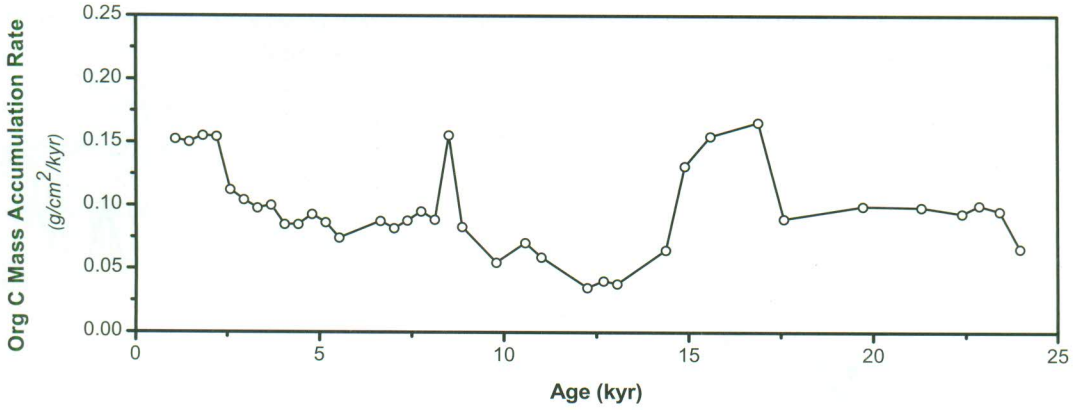

Fig. 3. Mass accumulation rates (MARs) of organic carbon in core AAS 9/21.

core SK 157/20, new splits of cleaned *G. ruber* specimens (250 to 350 μm size range) were analyzed using a Finnigan MAT 252 mass spectrometer equipped with an automatic carbonate preparation device at the Universität Bremen, Germany. Carbon isotopic values are calibrated against the NBS 18, 19, and 20 standards and are expressed as per mil (‰) versus the Vienna Pee Dee Belemnite (VPDB) standard. The mean external error and reproducibility (1σ) of carbonate standard is better than 0.05 for $\delta^{13}C$. Age models for the cores ODP 723A, AAS 9/21 and SK 218 were taken from earlier studies (Naidu and Niitsuma, 2004; Govil and Naidu, 2010, 2011).

Results and Discussion

The sediment cores presented in this paper span a great range in water depth (~800 m to 3300 m) and a wide geographical extent representing a range of Physico-chemical parameters. All these cores are from above the chemical lysocline depth at ~4000 m (Schulte and Bard, 2003). In core ODP 723A, collected from the Western Arabian Sea at a depth of 800 m, shell weights of *G. ruber* range from 12 to 19 μg for the last ~22 kyr (Fig. 2a). Shell weights show a decrease from the LGM to the period ~17.5 kyr, an increase during deglaciation and followed by another decrease through the Holocene. The sediment core AAS 9/21 was collected from the Eastern Arabian Sea (EAS) at a water depth of ~1800 m. Shell weights range from ~13–16 μg in this core. In general, there are no large variations in shell weights in this core, although heavy shell weights were noticed during deglaciation.

Core SK 218 recovered from a water depth of 3307 m from the Bay of Bengal (BoB) shows shell weights varying in the range 14–19 μg. Similar to other cores in this study, heavier shell weights were recorded for the period of deglaciation. Another core (SK 157/20) collected from the central BoB at a water depth of 3171 m presents a shell weights in the range 12–18 μg. Core SK 157/20 only covers the last 16 kyr, although it also documents greater shell weights during deglaciation than in the Holocene.

In general, the four cores from the northern Indian Ocean show similar variations in shell weight, with carbonate preservation during deglaciation evident through higher shell weights. The shell weight trends averaged across the four cores display higher average shell weight during the LGM, followed quickly by a decrease and a peak in shell weights around 16 kyr. There is then a gradual decrease through the Holocene (Fig. 2b). We believe that LGM and Holocene average shell weights do not show great variation (see Table 1). We calculated the mass accumulation rate (MAR) of organic carbon using the following formula with dry bulk density (DBD) calculated using the empirical equation of Curry and Lohmann (1986):

$$\text{Organic carbon MAR}\left(\frac{\frac{\text{g}}{\text{cm}^2}}{\text{kyr}}\right) = \text{Org C (\%)} * \text{sedimentation rate}\left(\frac{\text{cm}}{\text{kyr}}\right) * \text{DBD}\left(\frac{\text{g}}{\text{cm}^3}\right).$$

The MAR is seen to be high during the Late Holocene with the greatest values calculated for the carbonate preservation maximum (Fig. 3). High MARs suggest reduced exposure time to oxic conditions and hence reduced sedimentary organic matter respiration and a decrease in pore water dissolution (e.g., Higgins *et al.*, 2009).

Reduced atmospheric CO_2 levels during the period of glaciation were a result of CO_2 build-up in the deep ocean (Sigman and Boyle, 2000) causing a decrease in the levels of $[CO_3^{2-}]$ at depth. In the North Atlantic, the CO_3^{2-} change between the Last Glacial Maximum (LGM) and

Holocene has been observed to be negative for waters above a depth of ~3000 m and positive below that depth. This is likely due to a change in the geometry of the Atlantic Meridional Ocean Circulation (Yu *et al.*, 2010). In contrast, the LGM to Holocene CO_3^{2-} concentrations in the deep Indo-Pacific did not show a difference (Yu *et al.*, 2010). This lack of variation in LGM and Holocene CO_3^{2-} concentrations is also evident in our shell weight observations from across the northern Indian Ocean. The differences in shell weights during LGM and Holocene in all the cores presented here are within the limits of analytical error. Though there are a number of CO_3^{2-} reconstructions for the Atlantic and the Pacific oceans, there is published evidence from just a single core, WIND 28 K (Yu *et al.*, 2010) taken from the southwestern Indian Ocean and we could not find any observations for the deep and intermediate waters of the northern Indian Ocean.

We have observed maximum shell weights during deglaciation in all the cores measured as part of this study, which signifies that this is a carbonate preservation maximum. A similar feature is noticed extensively in the Atlantic and Pacific Oceans and is considered to be a global phenomenon. The reason for this is assumed to be due to an increase in deep-water CO_3^{2-} concentration during deglaciation by about 10 μmol/kg in the deep Atlantic, Indian, and Pacific oceans (Yu *et al.*, 2010). The deepwater CO_3^{2-} concentration increased during deglaciation, although surface CO_3^{2-} decreased (Yu *et al.*, 2010) which suggests the release of deep-sea CO_2 to the atmosphere via intermediate waters due to intensified upwelling (Anderson *et al.*, 2009). The main sites for CO_2 degassing were the equatorial Pacific and the Southern Ocean (Martínez-Botí *et al.*, 2015). The Arabian Sea also may be an important site for CO_2 degassing as excess CO_2 was observed in the eastern Arabian Sea during the Bølling Allerød (Naik *et al.*, 2015). The authors believe the northern Indian Ocean is an important location representing unique seasonality as both source and sink of CO_2. The authors believe that it merits detailed study to understand CO_2 degassing during LGM and deglaciation as CO_2 release increases carbonate burial in deep-sea sediments due to elevated CO_3^{2-} in the deep sea during deglaciation (Yu *et al.*, 2010). In the earlier literature this effect has only been seen at water depths greater than 1200 m. However this study documented higher shell weights and thus elevated CO_3^{2-} at shallower depths beginning at ~800 m.

Evidence for a deglacial peak in $CaCO_3$ preservation was described more than three decades ago (Berger, 1977), and corroborating results have appeared subsequently (e.g., Broecker *et al.*, 2001; Broecker and Clark, 2003; Jaccard *et al.*, 2009, 2010). However, the evidence is building from a growing number of sites across the globe where the expected deglacial peak in $CaCO_3$ preservation has not been found, raising doubts about the ventilation hypothesis (Anderson *et al.*, 2009; Mekik *et al.*, 2012). The lack of an observable $CaCO_3$ maximum during deglaciation is considered to be due to factors such as change in the ratio of organic carbon to $CaCO_3$ reaching the seabed, changes in ocean circulation patterns, and changes in sediment focusing (Mekik *et al.*, 2012). However Mekik *et al.* (2012) only took observations from one Indian Ocean core and it was located outside of the northern Indian Ocean. Our study provides evidence that the deglacial carbonate peak is seen in cores from the Arabian Sea as well as the BoB and across a range of water depths.

The *G. ruber* $\delta^{13}C$ record for the three cores (AAS 9/21, SK 218 and SK 157/20) is presented here (Fig. 2c). The $\delta^{13}C$ variations are within 0.5 to 1.6‰. The trend is almost linear throughout the 25 kyr record except for low $\delta^{13}C$ during early deglaciation. This is in line with the carbonate preservation spike (Fig. 2c). Such low $\delta^{13}C$ values have been observed globally in planktic and benthic foraminifera from intermediate depth during deglaciation and are thought to indicate upwelling of a nutrient enriched water mass of Southern Ocean origin, following renewed upwelling in that region due to earlier deglaciation (see Spero and Lea, 2002 and references therein; Anderson *et al.*, 2009; Naik *et al.*, 2015). The present study gives an indication that carbonate preservation during deglaciation was truly a global phenomenon and thus supports the ventilation hypothesis. This study highlights the role of the northern Indian Ocean in atmospheric CO_2 rise during deglaciation.

Conclusion

Shell weight record from four cores across the northern Indian Ocean shows a prominent spike in carbonate preservation in support of the ventilation hypothesis. It also highlights the role of the northern Indian Ocean in this process and the need to understand the so far unstudied deep-water carbonate chemistry of this region.

Acknowledgments—We are thankful to ODP for supplying the core samples and Ms. Priya Kolwankar and Mr. Vijay Toraskar who were responsible for shell weight measurements of sediment cores SK 218 and SK 157/20. This study forms a part of the GEOSINKS programme. This is NIO contribution No. 5871.

References

Anderson, R. F., Ali, S., Bradtmiller, L. I., Nielsen, S. H. H., Fleisher, M. Q., Anderson, B. E. and Burckle, L. H. (2009) Wind driven upwelling in the Southern Ocean and the deglacial rise in atmospheric CO_2. *Science* **323**, 1443–1446, doi:10.1126/science.1167441.

Archer, D. and Maier-Reimer, E. (1994) Effect of deep sea sedi-

mentary calcite preservation on atmospheric CO_2 concentration. *Nature* **367**, 260–263.

Berger, W. (1973) Deep-sea carbonate: Pleistocene dissolution cycles. *J. Foram. Res.* **3**, 187–195.

Berger, W. (1977) Deep-sea carbonate and the deglaciation preservation spike in pteropods and foraminifera. *Nature* **269**, 301–303.

Broecker, W. S. and Clark, E. (2003) Holocene atmospheric CO_2 increase as viewed from the seafloor. *Global Biogeochem. Cycles* **17**(2), 1052, doi:10.1029/2002GB001985.

Broecker, W., Lynch-Stieglitz, J., Clark, E., Hajdas, I. and Bonani, G. (2001) What caused the atmosphere's CO_2 content to rise during the last 8,000 years? *Geochem. Geophys. Geosyst.* **2**, doi:10.1029/2001GC000177.

Curry, W. B. and Lohmann, G. P. (1986) Late Quaternary carbonate sedimentation at the Sierra Leone Rise (eastern equatorial Atlantic Ocean). *Mar. Geol.* **70**, 223–250.

Denton, G. H., Heusser, C. J., Lowell, T. V., Moreno, P. I., Andersen, B. G., Heusser, L. E., Schluchter, C. and Marchant, D. R. (1999) Interhemispheric linkage of paleoclimate during the last glaciation, *Geogr. Ann., Ser. A, Phys. Geogr.* **81A**, 107–153.

Emerson, S. and Bender, M. (1981) Carbon fluxes at the sediment-water interface of the deep sea: calcium carbonate preservation. *J. Mar. Res.* **39**, 139–162.

Govil, P. and Naidu, P. D. (2010) Evaporation-precipitation changes in the eastern Arabian Sea for the last 68 ka: Implications on monsoon variability. *Paleoceanography* **25**, PA1210, doi:10.1029/2008PA001687.

Govil, P. and Naidu, P. D. (2011) Variations of Indian monsoon precipitation during the last 32 kyr reflected in the surface hydrography of the western Bay of Bengal. *Quat. Sci. Rev.* **30**, 3871–3879, doi:10.1016/j.quascirev.2011.10.004.

Higgins, J. A., Fisher, W. W. and Schrag, D. P. (2009) Oxygenation of the ocean and sediments: Consequences for the seafloor carbonate factory. *Earth Planet. Sci. Lett.* **284**, 25–33, doi:10.1016/j.epsl.2009.03.039.

Jaccard, S. L., Galbraith, E. D., Sigman, D. M., Haug, G. H., Francois, R., Pedersen, T. F., Dulski, P. and Thierstein, H. R. (2009) Subarctic Pacific evidence for a glacial deepening of the oceanic respired *carbon pool. Earth Planet. Sci. Lett.* **277**, 156–165, doi:10.1016/j.epsl.2008.10.017.

Jaccard, S. L., Galbraith, E. D., Sigman, D. M. and Haug, G. H. (2010) A pervasive link between Antarctic ice core and subarctic Pacific sediment records over the past 800 kyrs. *Quat. Sci. Rev.* **29**, 206–212, doi:10.1016/j.quascirev.2009.10.007.

Lohmann, G. P. (1995) A model for variation in the chemistry of planktonic foraminifera due to secondary calcification and selective dissolution. *Paleoceanography* **10**, 445–447.

Luthi, D., Le Floch, M., Bereiter, B., Blunier, T., Barnola, J.-M., Siegenthaler, U., Raynaud, D., Jouzel, J., Fischer, H., Kawamura, K. and Stocker, T. F. (2008) High resolution carbon dioxide concentration record 650,000–800,000 years before present. *Nature* **453**, 379–382, doi:10.1038/nature06949.

Marcott, S. A., Bauska, T. K., Buizert, C., Steig, E. J., Rosen, J. L., Cuffey, K. M., Fudge, T. J., Severinghaus, J. P., Ahn, J., Kalk, M. L., McConnell, J. R., Sowers, T., Taylor, K. C., White, J. W. C. and Brook, E. J. (2014) Centennial-scale changes in the global carbon cycle during the last deglaciation. *Nature* **514**, 616–621, doi:10.1038/nature13799.

Martínez-Botí, M. A., Marino, G., Foster, G. L., Ziveri, P., Henehan, M. J., Rae, J. W. B., Mortyn, P. G. and Vance, D. (2015) Boron isotope evidence for oceanic carbon dioxide leakage during the last deglaciation. *Nature* **518**(7538), 219–222, doi:10.1038/nature14155.

Mekik, F. A., Anderson, R. F., Loubere, P., François, R. and Richaud, M. (2012) The mystery of the missing deglacial carbonate preservation maximum. *Quat. Sci. Rev.* **39**, 60–72, doi:10.1016/j.quascirev.2012.01.024.

Naidu, P. D. and Niitsuma, N. (2004) Atypical $\delta^{13}C$ signature in *Globigerina bulloides* at the ODP Site 723A: implications of environmental changes caused by upwelling. *Mar. Micropaleontol.* **53**, 1–10, doi:10.1016/j.marmicro.2004.01.005.

Naik, S. S. and Naidu, P. D. (2014) Boron/calcium ratios in *Globigerinoides ruber*: Implications for controls on boron incorporation. *Mar. Micropal.* **107**, 1–7, doi:10.1016/j.marmicro.2014.01.004.

Naik, S. S., Naidu, P. D., Foster, G. L. and Martínez-Botí, M. A. (2015) Tracing the strength of the southwest monsoon using boron isotopes in the eastern Arabian Sea. *Geophys. Res. Lett.* **42**, 1450–1458, doi:10.1002/2015GL063089.

Rink, S., Kühl, M., Bijima, J. and Spero, H. J. (1998) Microsensor studies of photosynthesis and respiration in the symbiotic foraminifer, *Orbulina universa. Mar. Biol.* **131**, 583–595.

Schulte, S. and Bard, E. (2003) Past changes in biologically mediated dissolution of calcite above the chemical lysocline recorded in Indian Ocean sediments. *Quat. Sci. Rev.* **22**, 1757–1770, doi:10.1016/S0277-3791(03)00172-0.

Sigman, D. M. and Boyle, E. A. (2000) Glacial/interglacial variations in atmospheric carbon dioxide. *Nature* **407**, 859–869, doi:10.1038/35038000.

Spero, H. J. and Lea, D. W. (2002) The cause of carbon isotope minimum events on glacial terminations. *Science* **296**, 522–525, doi:10.1126/science.1069401.

Stuiver, M. and Reimer, P. J. (1993) Extended ^{14}C data base and revised CALIB 3.0 ^{14}C age calibration program. *Calibration 1993* (Stuiver, M., Long, A. and Kra, R. S., eds.), *Radiocarbon* **35**(1), 215–230.

Yu, J., Broecker, W. S., Elderfield, H., Jin, A., McManus, J. and Zhang, J. (2010) Loss of carbon from the deep sea since the Last Glacial Maximum. *Science* **330**, 1084–1087, doi:10.1126/science.1193221.